

SLIDING IN NONSMOOTH DYNAMICAL SYSTEMS, ITS ORIGIN AND CONSEQUENCES

M. R. JEFFREY*

May 5, 2010

Abstract. A hybrid dynamical system with sliding is derived from a smooth n -dimensional vector field. It approximates the dynamics of the smooth vector field whose precise form inside some ‘pinch’ zone can be approximated by the hybrid between a map, that effectively removes the pinch zone from the phase space, and a sliding vector field, that approximates the removed dynamics. Hybrid sliding systems are shown to generalise piecewise-smooth flows with sliding (so-called Filippov systems), in a manner that allows the origin of sliding behaviour to be traced back to smooth dynamical systems. We analyse examples that illustrate this, revealing how phenomena such as canards and bifurcations in smooth systems, are related to sliding bifurcations and other discontinuity-induced-bifurcations in nonsmooth systems. The method provides a heuristic explanation for catastrophic behaviour in an experimental superconductor device.

1. Introduction. The purpose of this paper is to make sense of certain catastrophic and nondeterministic behaviours that have recently been observed in generic dynamical systems with sliding. Sliding occurs in systems of ordinary differential equations that are piecewise-smooth, that is, smooth over regions of phase space, separated by *switching manifolds* where discontinuities occur. Sliding describes solution trajectories that become constrained to evolve along the switching manifold.

The prevailing convention for dynamics at a switching manifold was defined by Filippov [9], and finds ever more application across engineering, physics, economics and biology (see for example [4, 3, 10, 14, 15, 17]). Filippov’s definition has a physical interpretation as the convex combination of the vector fields either side of a discontinuity [9], and is equivalent to the Utkin method of equivalent control [27].

Consider an ordinary differential equation of the form

$$\dot{x} = f(x), \tag{1.1}$$

where the righthand-side is a piecewise-smooth function given by

$$f(x) = \begin{cases} f_i(x) & \text{if } x \in R_i, \\ F_{ij}(x) & \text{if } x \in \bar{R}_i \cup \bar{R}_j, \end{cases} \tag{1.2}$$

comprised of smooth vector-valued functions $f_i \in \mathbb{R}^n$, which apply on disjoint open regions $R_i \subset \mathbb{R}^n$. On the boundaries between adjacent regions R_i and R_j , where the closures \bar{R}_i and \bar{R}_j of R_i and R_j overlap, we assign set-valued functions

$$F_{ij} = \left\{ \frac{1+\lambda}{2} f_i + \frac{1-\lambda}{2} f_j : -1 < \lambda < 1 \right\}. \tag{1.3}$$

The union of the boundaries $\bar{R}_i \cup \bar{R}_j$ for all i, j , is the switching manifold. If the set F_{ij} contains a vector lying in the tangent plane of the switching manifold, we follow Filippov [9] in saying that an orbit of (1.1) *slides* along the manifold. The set of such points forms a submanifold which we call the sliding region.

A sliding region is called stable or unstable if orbits are attracted to it respectively in forwards or backwards time. The boundaries of sliding regions are called *folds* (where orbits in R_i or R_j are tangent to the manifold, hence they fold towards or away from it). It is

¹Department of Engineering Mathematics, University of Bristol, Bristol BS8 1TR, United Kingdom.

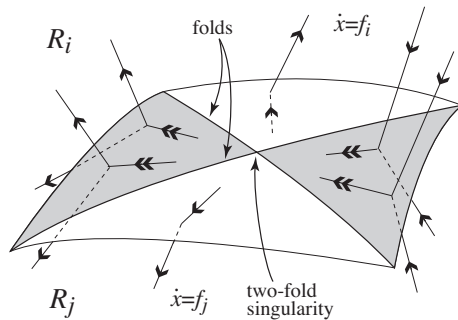


FIG. 1.1. Depiction of piecewise-smooth system showing a two-fold singularity in \mathbb{R}^3 . Orbits in the regions R_i and R_j are respectively solutions of $\dot{x} = f_i$ or $\dot{x} = f_j$. The differential equation is discontinuous on the switching manifold where orbits may either cross (unshaded surface) or slide (shaded surface). Sliding orbits (double arrows) are shown in stable (right) and unstable (left) sliding regions. These are bounded by curves called folds, which can cross to form a two-fold singularity.

possible for stable and unstable sliding regions to meet where a pair of folds intersect, and this important singularity is called a *two-fold* singularity (illustrated in figure 1.1). The two-fold has been the subject of ongoing interest, from the derivation of its normal form vector field [9], to the study of its asymptotic and structural stability [25, 11], both in \mathbb{R}^3 , and its role as a collision of folds in \mathbb{R}^2 [14].

The intrigue of the two-fold arises because it generates nondeterminism. Forward time evolution is nonunique from any point in an unstable sliding region on $\bar{R}_i \cup \bar{R}_j$, because each trajectory has infinitely many orbits departing from it into R_i and R_j in *finite* time. In many situations this behaviour is not of interest because orbits only flow away from the unstable sliding region. At a two-fold, however, the unstable sliding region adjoins a stable sliding region, where infinitely many orbits from R_i and R_j converge onto each sliding orbit in finite time. It is possible for trajectories to pass through the two-fold from the stable sliding region and access the unstable sliding region in forward time, so that orbits that converge on the two-fold are nondeterministic.

The two-fold is also central to a recent classification of a catastrophic class of *sliding bifurcations*. These are topological changes to invariant manifolds induced by a discontinuity. Previously known ‘regular’ types of sliding bifurcation [?] describe how changing a parameter causes a periodic orbit to attach to (or detach from) a switching manifold, gaining (or losing) a segment of sliding. In contrast, in a catastrophic sliding bifurcation, a periodic orbit will be destroyed suddenly without any precursive change in its stability or period.

Piecewise-smooth vector fields of the form (1.2) are often used to approximate smooth dynamical systems. The question therefore arises as to how the nondeterministic and catastrophic dynamics described above can be understood in the context of smooth systems.

A procedure to smooth out discontinuities has been devised, at least partially, and is known as regularization. To regularize the discontinuity at $\bar{R}_i \cup \bar{R}_j$ we introduce a transition region between R_i and R_j , foliated by surfaces $\lambda = \text{constant}$. By fixing $x \in \bar{R}_i \cup \bar{R}_j$ and varying λ between -1 and $+1$, we can let f assume unique values taken from the set F_{ij} in (1.3). The regularized system is topologically equivalent to a (smooth) singularly perturbed system, such that regions of sliding (defined by Filippov [9]) on the switching manifold are shown to be homeomorphic to hyperbolic slow manifolds (defined by Fenichel [8]) of the singularly perturbed system [26].

The requirement of hyperbolicity means that, if the slow manifold of the regularization is not hyperbolic, equivalence between a piecewise-smooth system and a singularly perturbed

system cannot be established. Nonhyperbolic points of slow manifolds have been the subject of recent interest relating to the phenomenon of canard explosion (see for instance [2, 23, 28]).

The current paper establishes a correspondence between two-folds and nonhyperbolic points of slow manifolds. That is, we show that two-fold singularities in piecewise-smooth vector fields approximate the dynamics around nonhyperbolic points of critical manifolds in singularly perturbed vector fields. To do this we derive a hybrid dynamical system that approximates the singular perturbation. Given a smooth vector field, and a certain *pinch zone* (where the dynamics is rapidly varying in time or phase space), we show that its dynamics can be approximated by a piecewise-smooth system of the general form in (1.1)-(rhs). The vector field in the pinch zone is replaced by a set valued vector field, and we show how approximating this as a convex set results in Filippov's convention (1.3). We prove that fixed points in the smooth and piecewise-smooth systems are in direct correspondence. It remains an open problem to establish whether there is a topological equivalence between smooth and nonsmooth systems, though one of continuing interest [16, 22].

The method is motivated by the pinching of a smooth vector field on a sphere [21]. In [22], the topology of hybrid representations of some nonsmooth systems was investigated, though the analysis excluded sliding, focusing on crossing dynamics such as the Zeno phenomenon. In contrast we will concentrate on the appearance of sliding and nondeterminism in hybrid approximations to dynamical systems.

The approximation method is introduced as a hybrid description of systems with sliding in section 2. In section 3 it is shown that a nonhyperbolic point on a slow manifold in \mathbb{R}^2 is approximated by the two-fold, using the classic example of the van der Pol oscillator. We also show, in a contrasting parameter regime, that the van der Pol oscillator displays a two-fold singularity called the fused focus [14]. A generic form of the two-fold is derived from the generic form of a nonhyperbolic slow manifold in \mathbb{R}^3 in section 4, and the catastrophic sliding bifurcations associated with it are discussed. Four catastrophic sliding bifurcations were classified in [12], three of which are related to the two-fold. In section 5 we discuss the fourth, and study what is, to my knowledge, the first occurrence of it identified in an experimental device – the superconducting resonator. The mathematical model of this device that has proven difficult to understand with either nonsmooth or smooth models alone, and using heuristic results from section 2, we make qualitative predictions about its operation. Some closing remarks are made in section 6.

2. A hybrid dynamical system with sliding. In this section we describe a method for replacing a smooth vector field by a hybrid of two vector fields and a map. By derive a particular form for the hybrid, and then show that it can be further approximated by a convex solution equivalent to Filippov's convention for a piecewise-smooth system.

Consider a smooth vector field $f : \mathbb{R}^n \mapsto \mathbb{R}^n$ that defines a dynamical system $\dot{x} = f(x)$. On some neighbourhood $\mathcal{U} \subset \mathbb{R}^n$, let there exist a smooth scalar function $h : \mathbb{R}^n \mapsto \mathbb{R}$ such $h'(x) \neq 0$ for all $x \in \mathcal{U}$. Let h have two level sets labeled

$$\Sigma_{\pm} = \{x \in \mathbb{R}^n : h(x) = \pm\sigma\}, \quad (2.1)$$

for some $\sigma > 0$, bounding a strip $|h| < \sigma$ which we call the *pinch zone*. We shall denote by \dot{h} the Lie derivative of h along the flow, given by

$$\dot{h} = \dot{x} \cdot \frac{d}{dx}h(x) = f \cdot \nabla h. \quad (2.2)$$

We wish now to replace the solutions of $\dot{x} = f$ in the pinch zone by some rule that: (i) associates each point on Σ_+ with a point on Σ_- , and (ii) replaces the vector field between them by a suitable approximation.

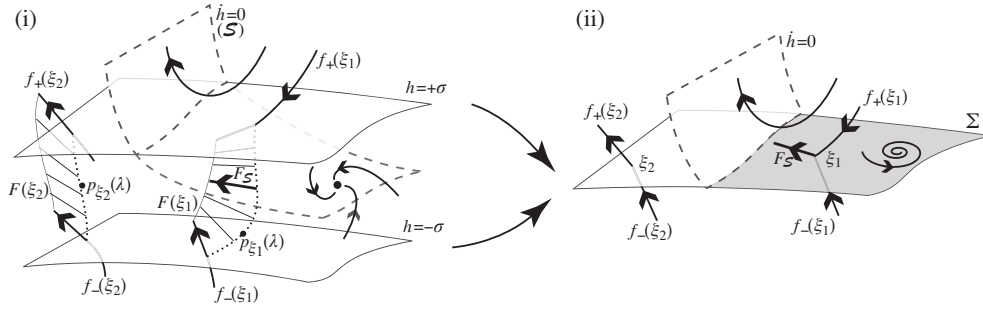


FIG. 2.1. A hybrid system with sliding. (i) In a smooth vector field f we add a pinch zone, bounded by Σ_{\pm} which are joined by chords $p_{\xi}(\lambda)$, on which the set-valued vector field $F(\xi)$ is shown at a sliding point ξ_1 and a crossing point ξ_2 . Sliding is determined by the positioning of a tangency surface $\dot{h} = 0$ (S in Theorem 2.1), on which we take the sliding vector F_S . A fixed point in the pinch zone is also shown. (ii) Hybrid system where Σ_+ and Σ_- pinch down to a switching manifold Σ . The tangency to Σ bounds sliding (shading) and crossing (unshaded) on Σ .

Locally in \mathcal{U} , we can define a surjective map from the pinch zone $|h(x)| < \sigma$, to a switching manifold $\Sigma \subset \mathbb{R}^{n-1}$. Geometrically, we connect each point $x_- \in \Sigma_-$ to a point $x_+ \in \Sigma_+$, by a smooth chord inside the pinch zone such that no two chords intersect. Let $p_{\xi}(\lambda)$ define the chord such that $p_{\xi}(-1) = x_-$ and $p_{\xi}(+1) = x_+$, where $\xi \in \Sigma$. Two such chords are illustrated in figure 2.1. The vector field at ξ on Σ is then the set

$$F(\xi) = \{f(p_{\xi}(\lambda)) : -1 < \lambda < 1\}. \quad (2.3)$$

We do not need this whole set to prescribe dynamics on Σ . For simplicity we assume that, at any ξ , the set $F(\xi)$ contains at most one vector tangent to a level set of h , which we call a *sliding vector* and denote as

$$F_S(\xi) = \left\{f(p_{\xi}(\lambda)) : \dot{h}(p_{\xi}(\lambda)) = 0, \lambda \in (-1, 1)\right\}. \quad (2.4)$$

For this to be possible we must have that, for a given ξ , the chord $p_{\xi}(\lambda)$ is never tangent to the hypersurface $\dot{h} = 0$. This means that p must satisfy

$$0 \neq \frac{\partial}{\partial \lambda} \dot{h}(p_{\xi}(\lambda)) = \frac{\partial p_{\xi}(\lambda)}{\partial \lambda} \cdot \nabla(f(p_{\xi}(\lambda)) \cdot \nabla h(p_{\xi}(\lambda))). \quad (2.5)$$

If $F(\xi)$ contains a sliding vector, $F_S(\xi)$, then we describe ξ as a *sliding point*, otherwise it is a *crossing point* (Figs. 2.2(a-b)). Over any open region of sliding points, the sliding vectors constitute an $n - 1$ dimensional vector field, and thus a dynamical system on Σ given by

$$\dot{\xi} = F_S(\xi). \quad (2.6)$$

A hybrid dynamical system is defined as the concatenation of solutions of equation (2.6) on Σ , with solutions of $\dot{x} = f$ in the regions $h(x) > \sigma$ and $h(x) < -\sigma$. figure 2.2 illustrates typical dynamics in the smooth system with a pinch zone, and in the hybrid system as defined above. The following theorem discusses how tangencies to the pinch zone, and fixed points inside the pinch zone, appear in the hybrid system.

THEOREM 2.1. (i) The boundary between crossing and sliding lies where f is tangent to Σ_+ or Σ_- . (ii) Zeros of the vector field f inside the pinch zone correspond to zeros of the sliding vector field $F_S(\xi)$.

Proof. (i) Let \mathcal{S} denote the hypersurface on which $\dot{h} = 0$. Then \mathcal{S} is the set of points where f is tangent to a level set of h . A sliding point $\xi \in \Sigma$ exists when there exists $\lambda_* \in (-1, 1)$ such that $\dot{h}(p_\xi(\lambda_*)) = 0$, meaning that \mathcal{S} lies inside the pinch zone, otherwise ξ is a crossing point and \mathcal{S} lies outside the pinch zone since $|\lambda_*| > 1$. Assuming that h and f are smooth, the boundary between crossing and sliding is where \mathcal{S} departs the pinch zone at a point $x = p_\xi(\lambda)$ where $|\lambda| = 1$, meaning that $\dot{h}(p_\xi(\lambda)) = 0$ for $|\lambda| = 1$. Since $\dot{h} = f \cdot h$ and $h(p_\xi(\pm 1)) = \pm\sigma$, then f is tangent to one of the level sets $h = \pm\sigma$, which are the surfaces Σ_\pm . (ii) A zero of f inside the pinch zone means that $f(p_\xi(\lambda)) = 0$ for some $\lambda \in (-1, 1)$, therefore $\dot{h} = f \cdot h = 0$ at $x = p_\xi(\lambda)$, so ξ is a sliding point where the sliding vector field is $F_S(\xi) = f(p_\xi(\lambda)) = 0$. \square

At a sliding region, by time reversal we obtain orbits that either flow towards, or away from, the pinch zone. We describe this as stable (figure 2.2(a)) or unstable sliding, defined as:

DEFINITION 2.2. *The sliding vector field $F_S(\xi)$ is stable if $\dot{h}(p_\xi(+1)) > 0 > \dot{h}(p_\xi(-1))$, and unstable if $\dot{h}(p_\xi(-1)) > 0 > \dot{h}(p_\xi(+1))$.*

At a tangency, depending on whether the vector field curves away from or towards the pinch zone, we obtain visible (figure 2.2(d)) or invisible tangencies, defined as:

DEFINITION 2.3. *If an orbit lying outside the pinch zone is tangent to the boundary we say the tangency is visible, if it lies inside the pinch zone we say it is invisible. In the corresponding Filippov system it is common to call such a tangency a fold.*

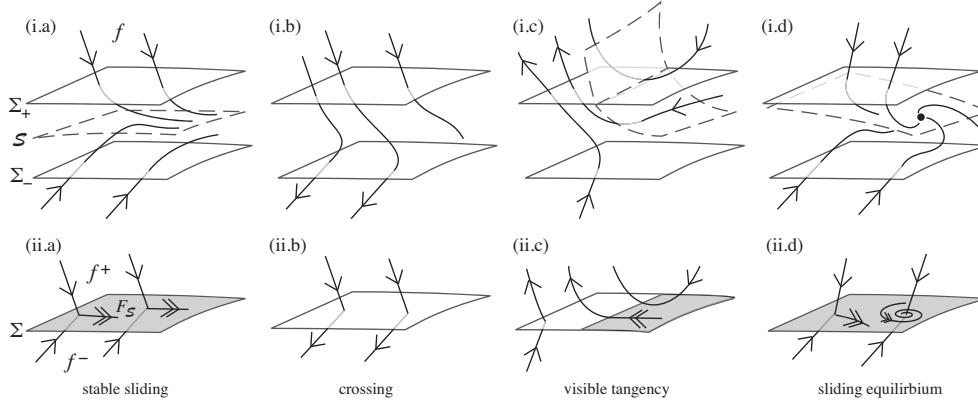


FIG. 2.2. *Some corresponding dynamics in (i) smooth and (ii) hybrid systems, obtained by pinching (see figure 2.1). The cases illustrated are: (a) sliding, (b) crossing, (c) a sliding equilibrium, (d) a tangency (or fold). The sliding depicted is stable, which reversing the direction of time changes to unstable.*

A sliding point, $\xi \in \Sigma$, corresponds to a chord $\{p_\xi(\lambda) : \lambda \in (-1, 1)\}$, on which the two orbits of $\dot{x} = f$ through the endpoints $p_\xi(\pm 1)$, flow either both outward or both inward with respect to the pinch zone, and connect to a sliding orbit in Σ . A crossing point corresponds to a chord on which the orbit of f at one endpoint flows into the pinch zone, and at the other flows outward, so that orbits cross through the region via a single point on Σ .

The codimension one surface \mathcal{S} defined in the proof to Theorem 2.1, is the set of points where $\dot{h} = 0$. Intersection of \mathcal{S} with Σ_\pm creates a fold (tangency, Def. 2.3) on codimension two surfaces in Σ , which partition Σ into regions of sliding or crossing. The domain of sliding is the set of points

$$x \in \{\mathcal{S} \cap \{x : |h(x)| < \sigma\}\}.$$

We conclude this section by deriving Filippov's convention as a natural approximation to hybrid sliding. Equation (2.6) requires knowledge of the exact form of the vector field f

inside the pinch zone, but consider if f is known only approximately outside the pinch zone and unknown inside it. We can approximate the set $F(\xi)$ for a point $\xi \in \Sigma$, (recalling that it contains the values of $f(x)$ along the chord $x = p_\xi(\lambda)$), by interpolating between the values of f at the endpoints $p_\xi(\pm 1)$, which gives $F(\xi) \approx \tilde{F}(\xi)$, where

$$\tilde{F}(\xi) = \left\{ \frac{1+\lambda}{2} f(p_\xi(+1)) + \frac{1-\lambda}{2} f(p_\xi(-1)) : -1 < \lambda < 1 \right\}. \quad (2.7)$$

This is precisely the convex combination of the vectors $f_\pm(\xi) = f(p_\xi(\pm 1))$ used by Filippov [9] to define sliding. A sliding vector, which lies on the surface \mathcal{S} , is a member of \tilde{F} that satisfies $\tilde{F} \cdot \nabla h = 0$. Assuming that $\nabla h(p_\xi(+1)) \approx \nabla h(p_\xi(-1))$, this occurs at $\lambda = \lambda_{\mathcal{S}}$, where

$$\lambda_{\mathcal{S}} = \frac{(f_- + f_+) \cdot \nabla h}{(f_- - f_+) \cdot \nabla h},$$

and thus the sliding vector field is

$$\tilde{F}_{\mathcal{S}} = \frac{(f_- \cdot \nabla h) f_+ - (f_+ \cdot \nabla h) f_-}{(f_- - f_+) \cdot \nabla h}, \quad (2.8)$$

which is Filippov's sliding vector field. Letting $\dot{h}_\pm(\xi) = \dot{h}(p_\xi(\pm 1))$, we can write this as

$$\tilde{F}_{\mathcal{S}}(\xi) = \frac{\dot{h}_-(\xi) f_+(\xi) - \dot{h}_+(\xi) f_-(\xi)}{\dot{h}_-(\xi) - \dot{h}_+(\xi)}. \quad (2.9)$$

The derivation of a Filippov system here can be thought of as a converse to the method of regularization [26]. There, a piecewise-smooth vector field with $f = f_+$ on $h > 0$ and $f = f_0$ on $h < 0$ is smoothed out by inserting a strip between the two half-spaces, so effectively $f = f_+$ on $h > \sigma$ and $f = f_0$ on $h < -\sigma$, then introducing a vector field F_ϵ on $|h| < \sigma$ that interpolates between the two,

$$\tilde{F}_\sigma(x) = \frac{1 + \lambda(h(x)/\sigma)}{2} f_+ + \frac{1 - \lambda(h(x)/\sigma)}{2} f_-(x), \quad (2.10)$$

where now $\lambda = \lambda(\nabla h \cdot x/\epsilon)$ is a monotonic function satisfying $\lambda(s)$ is equal to $+1$ if $s > 1$, to -1 if $s < -1$. In [] it is shown that the surface \mathcal{S} , described above, is homeomorphic to the slow manifold of a singular perturbation problem with small parameter σ . This, however, applies only if \mathcal{S} is hyperbolic. Points where this is violated are generic both in singularly perturbed systems and in nonsmooth systems. We discuss what these are, and their importance to both dynamical regimes, in the following sections.

3. The two-fold singularity in \mathbb{R}^2 . Before considering the generic two-fold singularity in section 4, which requires three dimensions, let us consider a classic planar system in which they arise, namely the van der Pol oscillator. This model of an oscillator with nonlinear damping separates into fast and slow timescales in the limit as the damping stiffness parameter approaches infinity. We will also show that what happens in the limit of small damping.

Consider the well studied Liénard form of the van der Pol oscillator,

$$\begin{pmatrix} \dot{x} \\ \dot{y} \end{pmatrix} = \begin{pmatrix} (y - \frac{1}{3}x^3 + x)/\epsilon \\ a - x \end{pmatrix}, \quad (3.1)$$

where a and ϵ are positive constants (negative a gives the same system with (x, y) replaced by $(-x, -y)$).

As is well known [[GuckHolmes??], the dynamical system (3.1) has a fixed point at $(x_{\text{eq}}, y_{\text{eq}}) = (a, \frac{1}{3}a^3 - a)$ which is stable if $|a| > 1$. If $|a| < 1$ the fixed point is unstable and enclosed by a stable periodic orbit. A Hopf bifurcation takes place when $a = 1$ (and also $a = -1$), that is, as the fixed point passes through the ‘knee’ $(x_{\text{H}}, y_{\text{H}}) = (1, -\frac{2}{3})$ of the curve $y = \frac{1}{3}x^3 - x$.

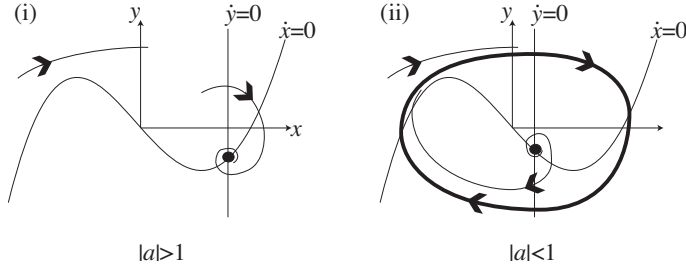


FIG. 3.1. The van der Pol oscillator in the Liénard plane for a moderate value of k .

3.1. $\epsilon \ll 1$, the canard, and the visible-invisible two-fold. In the stiff damping regime given by $\epsilon \ll 1$, instead of a Hopf bifurcation we obtain the well studied canard phenomenon [2, 7]. We describe this here using a hybrid sliding approximation as defined in section 2.

In the limit $\epsilon = 0$ the system (3.1) separates into subsystems with two different timescales. If we set $\epsilon = 0$, then on the curve $y - \frac{1}{3}x^3 + x = 0$ we can write down a dynamical system with $\dot{y} = a - x$. This one-dimensional *slow* subsystem has an equilibrium at $x = a$ which is repulsive if $a < 1$ and repulsive if $a > 1$, but is undefined at the turning points $x = \pm 1$. If we rescale time by $t \mapsto t/\epsilon$ we obtain the *fast* subsystem, for which $\dot{y} = 0$, and the curve $y - \frac{1}{3}x^3 + x = 0$ is a family of equilibria which are attracting on the branch where $|x| > 1$, and repulsive on the central branch where $|x| < 1$.

Let us therefore define the function $h(x, y) = y - \frac{1}{3}x^3 + x$, and define a pinch zone $|h| < \epsilon$ around the $\dot{x} = 0$ nullcline $h = 0$. The small value of ϵ makes the curve $h = 0$ strongly attracting for $|x| > 1$ and repelling for $|x| < 1$, figure 3.2(i.a). It also compresses the Hopf bifurcation into a cascade of orbits near $a = 1$, two of which are shown in figure 3.2(i.b), resulting in a periodic *relaxation oscillation* shown in figure 3.2(i.c). In the hybrid system the cubic curve is a switching manifold with stable sliding for $|x| > 1$ and unstable sliding for $|x| < 1$, figure 3.2(ii.a). The cascade is compressed into the instant $a = 1$, figure 3.2(ii.b), and represented by the existence of an infinite number of periodic orbits that contain canard segments – defined as solutions that pass from the stable to unstable branches of sliding on the switching manifold [?] – leaving behind the relaxation oscillation in figure 3.2(ii.c).

The bifurcation diagram is shown in figure 3.2(iii); note the vertical gradient at the non-smooth Hopf bifurcation that corresponds to a canard explosion.

The hybrid system can be derived by taking a pinch zone given by $|h| < \sigma$ for some $\sigma > 0$. Recall from section 2 that we then choose a map p from one of the pinch zone’s boundaries $|h| = \mp\sigma$ to the other, satisfying (2.5). For this we can choose simply the lines given by $p_x(y) = (x, \frac{1}{3}x^3 - x + \lambda\epsilon)$ for $-1 < \lambda < 1$.

If we then define a new coordinate $\tilde{y} = y - \sigma \text{sgn}[h(x, y)]$, we can express the vector

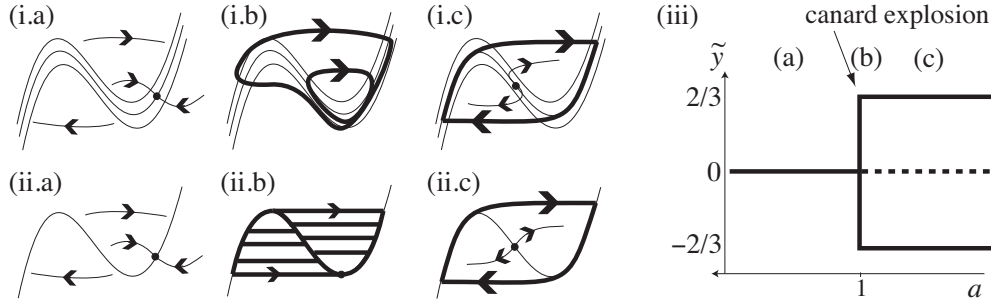


FIG. 3.2. Canard explosion in a van der Pol oscillator: (i) smooth system with a pinch zone around $|h| < \epsilon$, (ii) hybrid (or Filippov) system, (iii) bifurcation diagram. For (a) $a > 1$, (b) $a \approx 1$, (c) $a < 1$. In (i.b) two periodic orbits called canards “with head” (larger) and “without head” (smaller) are shown for different values of a close to unity. In (ii.b), an infinite number of periodic orbits coexist when $a = 1$.

field in (3.1) as

$$\begin{pmatrix} \dot{x} \\ \dot{y} \end{pmatrix} = \begin{pmatrix} \pm \frac{\sigma}{\epsilon} + \frac{1}{\epsilon} h(x, \tilde{y}) \\ a - x \end{pmatrix} \quad (3.2)$$

for $\tilde{y} - \frac{1}{3}x^3 + x \neq 0$, where ± 1 is the sign of $\tilde{y} - \frac{1}{3}x^3 + x$. Then we have a Filippov system comprised of the two vector fields (3.2) either side of the switching manifold $h(x, \tilde{y}) = 0$. Using (2.8) we find that the sliding vector field on the manifold is given by

$$\begin{pmatrix} \dot{x} \\ \dot{y} \end{pmatrix} = \begin{pmatrix} 1/(x^2 - 1) \\ a - x \end{pmatrix}, \quad \text{if } \frac{\sigma^2}{\epsilon^2}(1 - x^2)^2 - (a - x)^2 > 0. \quad (3.3)$$

The sliding vector field has an equilibrium at $x = a$, and is bounded by the folds at $\frac{\sigma^2}{\epsilon^2}(1 - x^2)^2 - (a - x)^2 < 0$. The folds can be seen in the magnification around the point $(1, -\frac{2}{3})$ shown in figure 3.3(i), and are labeled $T_{1,2}$. T_1 labels the lower vector field’s visible tangency (recall definition 2.3) to the switching manifold, and T_2 labels the upper vector field’s invisible tangency.

There are two regions $\frac{\sigma^2}{\epsilon^2}(1 - x^2)^2 - (a - x)^2 < 0$ where orbits cross the switching manifold, and these lie around the manifold’s turning points $\pm(1, -\frac{2}{3})$. In figure 3.3(ii) the crossing region is shown as a dotted curve.

Examining figure 3.3(ii) it is then easy to understand how the changing position of the fold points creates the local conditions that permit a periodic orbit to exist. The smooth system is shown in figure 3.3(i). Note the bifurcation of the $\dot{h} = 0$ nullcline \mathcal{S} in the smooth system, which corresponds to visible and invisible folds passing each other in the hybrid system.

Figure 3.4 shows a more general depiction of the bifurcation that has taken place as a passed through $a = 1$. This shows the locus of the folds crossing transversally to form a two-fold singularity.

Thus we have a qualitative description of a canard explosion, in terms of a bifurcation in a piecewise-smooth system. The family of canard cycles that make up a canard explosion are compressed from an exponentially small range of the parameter $a = 1$, into the instant $a = 1$. It is possible to make the analysis more precise, and resolve the different parameter values for which we have the canards with head and without head in figure 3.2 (i.b) or (ii.b). We do this by making a change of coordinates that lifts the focus out of the pinch zone into the upper vector field.

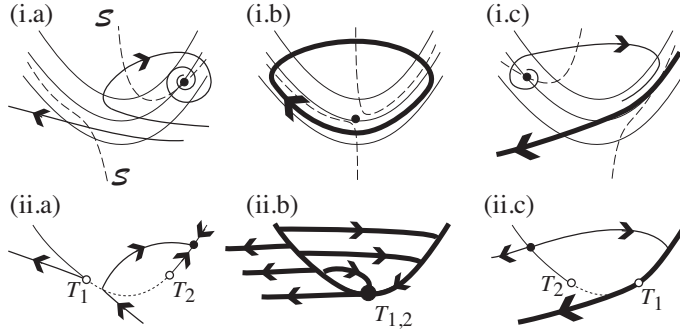


FIG. 3.3. Close-up of the knee of the curve $h = 0$ during the canard explosion, for (a) $a \lesssim 1$, (b) $a \approx 1$, (c) $a \gtrsim 1$. (i) in the smooth system, the equilibrium moves from the stable to unstable branch of the pinch zone (going from (i.a) to (i.c)), and the large periodic orbit (bold) shrinks, then is destroyed in a Hopf bifurcation. Note that the S curve $\dot{h} = 0$ (dashed) bifurcates. (ii) the canard explosion in the Filippov system, which takes place as folds T_1 and T_2 (where the vector field is tangent to the manifold) change ordering, and the sliding equilibrium changes sliding region. When they coincide in (b), sliding orbits can pass from the stable to unstable sliding region (canards), and they belong to infinitely many periodic orbits.

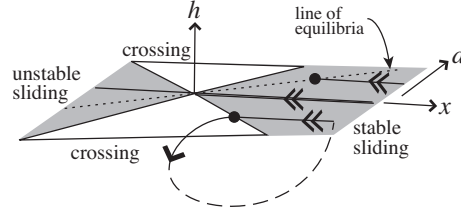


FIG. 3.4. Catastrophic bifurcation at a visible-invisible two-fold. A periodic orbit is shown leaving the stable sliding region of the switching manifold via a visible fold. The dashed line denotes some return mechanism, regardless of which, the periodic orbit will be destroyed by varying a so that the orbit passes through a two-fold.

The key to this is the form of the $\dot{h} = 0$ nullcline S . From (3.1) with $h = y - \frac{1}{3}x^3 + x$, this is given by $a - x + (1 - x^2)h/\epsilon = 0$, hence

$$S = \{(x, y) : h(X, y) = \epsilon(x - a)/(1 - x^2)\}. \quad (3.4)$$

At the bifurcation, when $a = 1$, this takes the form $\{(x, y) : h(x, y) = -\epsilon/(1 + x)\}$, which we denote S_0 . As observed in [2], the largest canard without head is the one which slides along the full length of the unstable sliding region (called a *maximal* canard), and this one can be approximated by S_0 whilst in the pinch zone. We therefore change coordinates to center on the curve S_0 , by defining $z = h(x, y) + \epsilon/(1 + x)$ and studying dynamics in the (x, z) plane.

In the (x, z) system for $\epsilon \ll 1$ there exists a normally hyperbolic slow manifold in a neighbourhood of the line $z = 0$. We introduce a new pinch region $|z| < \sigma'$ for some $\sigma' > 0$

3.2. The maximal canard and the visible two-fold. It was observed in [2], that during a canard explosion we can identify a *maximal canard* that separates the canards with head from those without head. As the parameter a changes, the maximal canard is the periodic orbit that separates the in the van der Pol oscillator that when the bifurcation occurs at $a = 1$, the canard trajectory that appears lies exactly along the critical surface S given by $\dot{h} = 0$. Evaluating $\dot{h} = \dot{y} + \dot{x}(1 - x^2) = a - x + kh(1 - x^2)$, we solve to find $h = h_S :=$

$(a - x)/k(x^2 - 1)$, which at $a = 1$ is

$$h = h_0 := -\frac{1}{k(1+x)}. \quad (3.5)$$

Following [Benoit] we can magnify the vector field around the trajectory $h = h_0$ by introducing a coordinate $w = (h(x, y) + h_0(x))^{1/k}$. The square bracket in the exponent denotes the operation defined as $u^{[p]} = |u|^p \text{sgn}(u)$.

$$\begin{aligned} \dot{x} &= k(w^{[k]} + h_0(x)) \\ \dot{w} &= w^{[1-k]} ([w^{[k]} + h_0(x)] [(1-x^2) - kh_0^2(x)] + (a-x)/k). \end{aligned} \quad (3.6)$$

By considering the limit $k \rightarrow \infty$ we see that this has a slow manifold in the neighbourhood of the line $w = 0$. Following the general procedure above we therefore define a pinch zone $|w| < \sigma$ for some $\sigma > 0$. The surface \mathcal{S} where $\dot{w} = 0$ is given by ...

with a repelling focus on \mathcal{S} where $w = (-h_0(x))^{1/k}$. We derive the hybrid approximation by introducing a new coordinate $v = w - \sigma \text{sgn}(w)$. We obtain (hopefully something like)

$$\dot{x} = x + v, \quad \dot{v} = v - x, \quad v > 0 \quad \dot{x} = -1, \quad \dot{v} = v, \quad v < 0. \quad + \text{ord}[\sigma, 1/k, w] \quad (3.7)$$

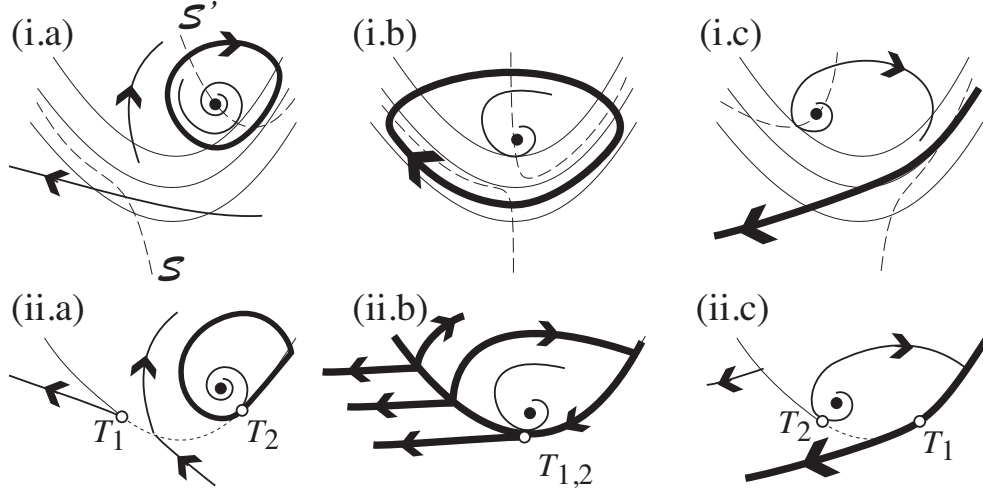


FIG. 3.5. The hybrid sliding system for figure 3.5, showing: (a) a periodic orbit entering the pinch zone (compare with figure ??(i-ii.b)), (b) the canard orbit, and bifurcation of \mathcal{S} , (c) no periodic orbits. A Filippov system and the catastrophic sliding bifurcation at a visible two-fold. (a) $\alpha < -1$, a stable periodic orbit (bold) and unstable focus. (b) $\alpha = -1$, the two visible folds coincide, infinitely many periodic orbits exist with canard segments. (c) $\alpha > -1$, no periodic orbits exist. As in previous sections, \mathcal{S} is the tangency set, here given by $\dot{y} = 0$.

then describe this bifurcation, which is:

The following sliding bifurcation has been classified only recently [12]. It predicts that a periodic orbit can be destroyed by a catastrophic sliding bifurcation at a visible two-fold, figure ??(vi), as depicted in figure 3.6.

It cannot be found in the typical slow-fast system of the form $(\epsilon\dot{x}, \dot{y}) = (f, g)$, because the trajectories bend the wrong way. And yet, surprisingly it does turn up in the van der Pol

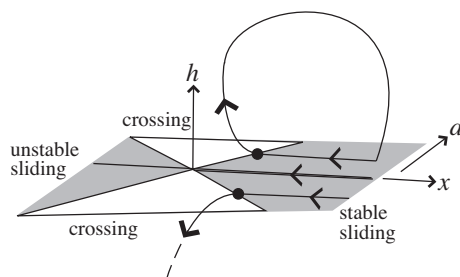


FIG. 3.6. Catastrophic bifurcation at a visible two-fold.

system under magnification, to allow the transition between canards with and without head. Here we present this briefly.

Here we give an explicit example of the bifurcation and, using the hybrid sliding formalism, we make sense of it as the approximation of a smooth nonlinear system.

Consider a Filippov system

$$\begin{pmatrix} \dot{x} \\ \dot{y} \end{pmatrix} = \begin{cases} f_+(x, y) & \text{if } y > 0, \\ f_-(x, y) & \text{if } y < 0, \end{cases}, \quad (3.8)$$

where

$$f_+(x, y) = \begin{pmatrix} y + \beta x - 1 \\ \beta y - x - 1 \end{pmatrix} \quad \text{and} \quad f_-(x, y) = \begin{pmatrix} -1 \\ x - a \end{pmatrix}, \quad (3.9)$$

for $\beta > 0$. figure 3.5 shows the basic dynamics, consisting of a switching manifold at $y = 0$, to which there are two visible tangencies: of the upper vector field at

$$x_{T+} = -1,$$

and the lower vector field at

$$x_{T-} = a.$$

Between the tangencies is a crossing region, with stable sliding to the right of it and unstable sliding to the left. The sliding vector field given by

$$\dot{x} = f_{sl}(x) = \frac{(\beta x - 1)(1 + x - a)}{1 + 2x - a}(1, 0) \quad \text{if } y = 0, (x - x_{T+})(x - x_{T-}) < 0. \quad (3.10)$$

There is an unstable focus at $(x_{eq}, y_{eq}) = (\beta - 1, \beta + 1)/(1 + \beta^2)$. For $a < -1$, the unique orbit leaving the tangency point $(x_{T+}, 0)$ wraps around the focus and returns to the stable sliding region, reconnecting to itself via a sliding orbit, thus forming a stable periodic orbit, shown in figure 3.5(a). (This can be easily verified by computing the explicit solutions for $y > 0$, $y < 0$, and $y = 0$ separately. Other invariant sets exist, but remain far outside the neighbourhood of the stable periodic orbit of interest if we fix $\beta \ll 1$).

The two tangencies coincide when $a = -1$, figure 3.5(b), so that a canard orbit exists, recalling that a canard in a Filippov system is a trajectory passing between stable and unstable sliding regions. The canard orbit is part of an infinite number of periodic orbits in the region $y \geq 0$. For $a > -1$ no periodic orbits exist, destroyed by the catastrophic sliding bifurcation at a visible two-fold.

The system suffers from having a nonunique solution at $a = -1$. We now show, however, by interpreting the Filippov system (3.8) as a hybrid sliding system in the manner of section 2, that the degeneracy of periodic orbits represents a canard explosion that arises somewhat differently to those of the van der Pol system (section ??).

We have added the $\dot{y} = 0$ critical surfaces comprising \mathcal{S} to figure 3.5 (shown dashed). We assume that these are part of a hybrid sliding system, derived from a smooth vector field in which \mathcal{S} is a smooth curve. If we choose the pinch function $p_\xi(\lambda)$ (see section 2) to consist simply of vertical chords, that is $p(\lambda; x) = (x, \lambda\sigma)$, then \mathcal{S} can take only the forms shown in figure ?. This follows from the assumption that \mathcal{S} only passes through the pinch zone in a sliding region, and that \mathcal{S} does not cross a vertical chord more than once (condition (2.5)). The important result is that, similar to the bifurcation responsible for the canard explosion in figure 3.3, the critical curve \mathcal{S} must undergo a bifurcation to get from figure ??(a) to ??(c).

The simplest smooth flow completing figure ?? and containing a stable periodic orbit is that in figure ??(a). It is impossible to construct a stable periodic orbit with finite period in figure ??(c). In (b), a bifurcation of the surface \mathcal{S} takes place at $a = -1$, and it is possible for a canard orbit to exist. The transition from (a) to (b) can be made by a canard explosion – a cascade of periodic orbits with rapidly increasing amplitude (note that the cascade must be increasing to infinity, rather than converging on the fixed point as in section ??, because the focus does not undergo a change in its stability).

Of course, this cascade solution is not unique, we could conceive of any number of different solutions for the flow inside the pinch zone that match the conditions at its boundary, however we are not concerned with the detailed dynamics inside the pinch zone, so long as the qualitative effect it has on the global dynamics is consistent with figure 3.8. It makes sense, therefore, to consider the simplest solution possible.

We can now construct a smooth system that exhibits this canard phenomenon. Consider the following regularisation of (3.8),

$$\begin{pmatrix} \dot{x} \\ \dot{y} \end{pmatrix} = \frac{1 + \phi(ky)}{2} f_+(x, y) + \frac{1 - \phi(ky)}{2} f_-(x, y) \quad (3.11)$$

where ϕ is a smooth function that switches rapidly from $\phi = -1$ to $\phi = +1$ as the argument ky changes sign. Such sigmoidal functions are common in models of systems with switching, such as neuron activation and control theory.

figure ?? shows a simulation of the system for different values of a around the value -1 , made in Mathematica [29] with $\phi = \tanh$ and $k = 4$. In each frame, two initial conditions are chosen, one in the top righthand corner and one near the focus, and where their orbits converge to a periodic solution a limit cycle is shown in bold.

An unstable focus exists above the pinch zone, and for small enough β it is surrounded by a stable periodic orbit if $a < -1$, figure ??(a), part of which lies inside the pinch zone ($y \approx 0$). Up to within -10^{-7} of $a = -1$, figure ??(b), Mathematica is able to compute orbits and show that the periodic orbit persists, growing rapidly in amplitude as a increases, constituting a canard explosion. Close to $a = -1$ the solutions cannot be computed robustly in the pinch zone. This indeed is why we use a nonsmooth approximation, and it leads to the orbits shown in figure ??(c), where different initial conditions lead unpredictably to solutions that evolve into either the $y > 0$ or $y < 0$ regions. For $a > -1$ and sufficiently far from $a = -1$ that orbits can be calculated robustly, figure ??(d) shows that no finite periodic orbit exists. This behaviour is consistent with the hybrid sliding interpretation, figure ??, of the catastrophic bifurcation in the Filippov system figure 3.5.

3.3. $k \ll 1$, the fused focus and the invisible two-fold. The contrasting case of $k \ll 1$ in equation (3.1) yields a pinch zone that is a vertical strip, and again always contains the

focus. The periodic orbit lies entirely within the pinch zone for $\sqrt{\alpha} < \sigma$, figure 3.7(i.a-b), and has two arcs outside it otherwise, figure 3.7(i.c). The figure shows a magnification on the right knee of the tangency curve \mathcal{S} , given in this case by the cubic nullcline $y = \frac{1}{3}x^3 - x$. The pinch zone is given by $|h| = |x - a| < \sigma$, and an appropriate thickness is $\sigma = k$.

A Filippov system is derived by defining a new coordinate $\tilde{x} = x - a - \sigma \text{sgn}[h]$, and it is convenient to introduce new coordinates,

$$\begin{aligned} u &= \frac{\sigma}{k}(x - a - \sigma \text{sgn}[h]) \\ v &= \sigma(y - \frac{1}{3}a^3 + a(1 - \sigma^2)) \end{aligned} \quad (3.12)$$

to obtain the vector fields outside of the switching manifold as

$$\begin{pmatrix} \dot{u} \\ \dot{v} \end{pmatrix} = \begin{pmatrix} v + \epsilon_0 u + (\epsilon u - \beta) \text{sgn}[u] + \mathcal{O}[k^2 u^2] \\ -\text{sgn}[u] + \mathcal{O}[ku] \end{pmatrix} \quad (3.13)$$

in terms of parameters $\beta = \frac{1}{3}\sigma^3 - \sigma(1 - a^2)$, $\epsilon_0 = k(1 - a^2 - \sigma^2)$, $\epsilon = -2a\sigma$.

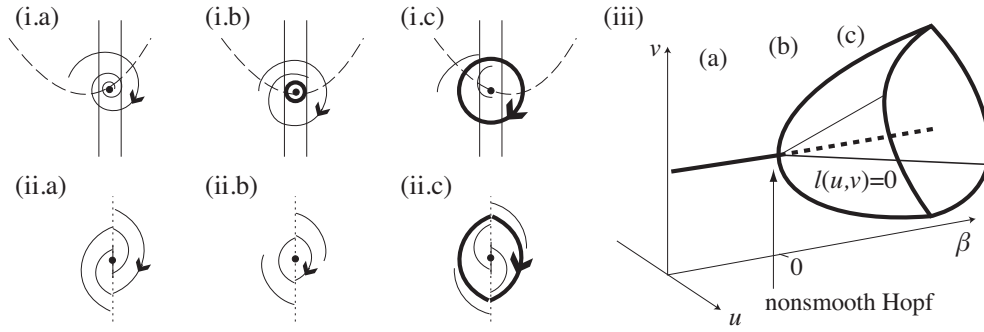


FIG. 3.7. The fused focus type of nonsmooth Hopf bifurcation: (i) hybrid system, (ii) Filippov system, (iii) bifurcation diagram with $l(u, v) = \frac{\beta}{\epsilon_0} - \frac{1}{2}(v + \frac{\beta}{\epsilon_0}\epsilon)^2 - |u|$.

There are two invisible folds at $v = \pm\beta$, with sliding between them on the switching manifold $u = 0$. The sliding vector field is $F_S = -v/\beta$ and has a fixed point at $v = 0$, which is stable for $\beta > 0$, figure 3.7(ii.a), and unstable for $\beta < 0$, figure 3.7(ii.c); this has previously been called a ‘fused focus’ [14]. At $\beta = 0$, figure 3.7(ii.b), the two invisible tangencies exchange ordering, which changes the stability of the sliding fixed point, creating a Hopf-like bifurcation. Because this is the only fixed point in the system we can neglect terms of order ku in the equation for \dot{v} (this does not change the sliding vector field), but they must be kept in the \dot{u} equation, without which the phase portrait is symmetric about the switching manifold $u = 0$ (and will therefore be a degenerate centre when $\beta = 0$).

Solutions of (3.13) satisfy (as can be proven directly by substitution into (3.13)),

$$\begin{aligned} |u| &= (\epsilon_{\pm}(\beta \mp v) + 1 - e^{\epsilon_{\pm}(\beta \mp v \mp u_0 \epsilon_{\pm})})/\epsilon_{\pm}^2 \\ &= |u_0| - \frac{1}{2}(v + u_0 \epsilon_0 + \text{sgn}[u](u_0 \epsilon - \beta))^2 + \mathcal{O}[3] \end{aligned} \quad (3.14)$$

where $\epsilon_{\pm} = \epsilon_0 \pm \epsilon$ with \pm denoting $\text{sgn}[u]$, and u_0 is a real parameter. The second line is a Taylor expansion to third order in the bracketed term $t = v + u_0 \epsilon_0 + \text{sgn}[u](u_0 \epsilon - \beta)$. The solutions are families of parabolic arcs as shown in figure 3.7(ii). Each arc intersects the switching manifold twice at points $v = v_1$ and $v = v_2$ which are roots of equation (3.14), given by

$$v_n^{\pm} = -u_0 \epsilon_0 \pm (\beta - u_0 \epsilon) + (-1)^n \sqrt{2|u_0|}, \quad (3.15)$$

where v_n^+ and v_n^- are solutions for the $u > 0$ and $u < 0$ systems respectively. A periodic orbit is formed when both of the conditions $v_1^+ = v_1^-$ and $v_2^+ = v_2^-$ are satisfied, which has only one solution, $|u_0| = u_{PO} \equiv \beta/\epsilon_0$. This means that a single periodic orbit exists and has equation

$$|u| = \frac{\beta}{\epsilon_0} - \frac{1}{2}\left(v + \frac{\beta}{\epsilon_0}\epsilon\right)^2 \quad (3.16)$$

obtained by putting $u_0 = \text{sgn}[u]u_{PO}$ into equation (3.14). Thus the periodic orbits exist for $\beta > 0$ (ϵ_0 is positive by definition), constituting the nonsmooth Hopf bifurcation shown in figure 3.7. The bifurcation diagram is shown in (iii); the size of the periodic orbit in the v -direction scales as $\sqrt{\beta}$, similar to a smooth Hopf bifurcation for a cycle of radius $\sqrt{\beta}$, while in the u -direction (parallel to Σ) it scales linearly with β .

4. The two-fold singularity in \mathbb{R}^3 . In 3D we prove an observation of M. Desroches, that Filippov vector fields at a two-fold resemble reduced vector fields of a singular perturbation problem at a nonhyperbolic point of a slow manifold...

Derive properly. So start from a generic non-hyperbolic point of a slow manifold

$$\begin{pmatrix} \dot{x} \\ \dot{y} \\ \dot{z}/k \end{pmatrix} = \begin{pmatrix} ay + bz \\ c \\ x - \frac{1}{2}z^2 \end{pmatrix} \quad (4.1)$$

$$h = x - \frac{1}{2}z^2 \quad (4.2)$$

and $|h| < \sigma$. Introduce $\tilde{x} = x - \sigma \text{sgn}(h(x, z))$,

$$\begin{pmatrix} \dot{\tilde{x}} \\ \dot{y} \\ \dot{z} \end{pmatrix} = \begin{pmatrix} ay + bz \\ c \\ k\sigma \text{sgn}(\tilde{x} - \frac{1}{2}z^2) + \mathcal{O}[\tilde{x} - \frac{1}{2}z^2] \end{pmatrix} \quad (4.3)$$

and taking the sliding vector field F_S on $\dot{h} = ay + bz - zk h = 0$ we have

$$\begin{pmatrix} \dot{y} \\ \dot{z} \end{pmatrix} = F_S = \begin{pmatrix} c \\ (ay + bz)/z \end{pmatrix} \quad \text{on} \quad \tilde{x} - \frac{1}{2}z^2 = 0. \quad (4.4)$$

Folds $0 = ay + bz \mp k\sigma z$ so $y = -z(b \mp k\sigma)/a$

$$zF_S = \begin{pmatrix} 0 & c \\ a & b \end{pmatrix} \begin{pmatrix} y \\ z \end{pmatrix}. \quad (4.5)$$

Straighten

$$\begin{pmatrix} \dot{\tilde{h}} \\ \dot{y} \\ \dot{z} \end{pmatrix} = \begin{pmatrix} ay + bz - kz\sigma \text{sgn}(\tilde{h}) \\ c \\ k\sigma \text{sgn}(\tilde{h}) \end{pmatrix} + \mathcal{O}[\tilde{h}] \quad (4.6)$$

From here we have 3 different types of canard. We also have a fourth catastrophic, pictured below (found in extending a classification of so-called sliding bifurcations). This was revealed recently in a superconductor recently. The question arises, can we use the hybrid interpretation to solve nonsmooth systems intuitively (that is using our intuition of

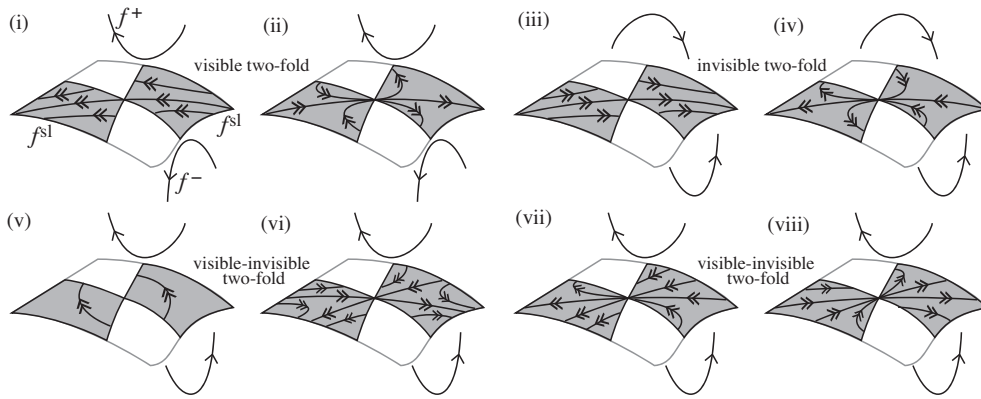


FIG. 4.1. The sliding vector field topologies at the two-folds. Shading regions are shaded. There are two topologies at a visible two-fold (i)-(ii) where $\alpha, \beta < 0$, two at an invisible two-fold (iii)-(iv) where $\alpha, \beta < 0$, and four at a visible-invisible two-fold (v)-(viii).

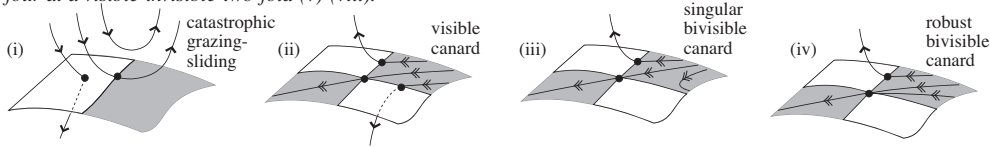


FIG. 4.2. The 4 catastrophic sliding bifurcations: a small change of inset causes a jump of outlet. (ii)-(iv) are reminiscent of canards in slow-fast systems.

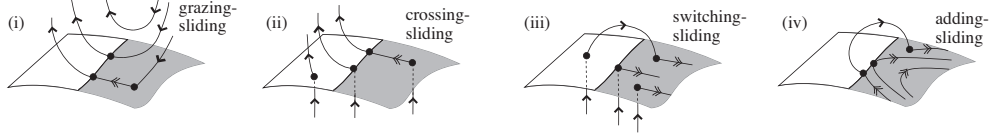


FIG. 4.3. The 4 sliding bifurcations: orbits transform continuously to gain or lose segments of stable sliding.

smooth systems) without explicitly regularising to an intractable smooth system? We try this next on the same.

The eight generic sliding bifurcations, (i)-(iv) the regular sliding bifurcation [4], (v)-(viii) the catastrophic sliding bifurcations [12]. In (vi)-(viii) a canard trajectory crosses from stable to unstable sliding via the point where two folds intersect. Reversing time changes stability of sliding (shaded) without altering the phase portrait. Cases (i),(ii),(v) occur at a visible fold (Fig ??(i)), (iii) occurs at an invisible fold (Fig ??(ii)), (iv) occurs at a visible cusp (Fig ??(iii)), and (vi)-(viii) occur at a two-fold.

5. Catastrophic sliding bifurcation in a superconducting resonator. We now consider a practical and rather more complicated problem, a three dimensional system that contains both singular perturbation and Filippov dynamics, which therefore cannot be solved by either of those two formalisms alone.

The superconducting resonator is an experimental device [20], designed as a sensor whose sensitivity could be controlled by laser heating of a niobium nitride (NbN) microbridge. The microbridge sits around the circumference of a conducting ring attached to a sensor probe. In experiment, however, novel self-sustained oscillations were observed [1, 20, 19, 18] with a simple physical origin, namely the oscillation of the microbridge between normal and superconducting states. At a low temperature the microbridge is superconducting, passing a high current which heats the bridge, until its temperature exceeds the threshold where it ceases to be superconducting, the current therefore decreases and the heating effect drops, so the bridge temperature falls below the threshold, the bridge becomes superconducting, and the process is seen to repeat periodically.

As a result, self-sustaining periodic oscillations are observed in the device's power output for certain experimental parameters. It was observed, however, that these oscillations could vanish suddenly, without prior change in period or amplitude, after which the system would settle to a stable fixed point in either the normal or superconducting temperature range.

The dynamical model proposed for the device [1, 10] can be expressed in terms of the power in the ring, which has complex amplitude β , and the temperature θ of the microbridge, satisfying

$$\begin{aligned}\dot{\beta} &= \Lambda\beta - i \\ \dot{\theta} &= -g\theta + s|\beta|^2.\end{aligned}\tag{5.1}$$

The parameters $s \in \mathbb{R}$ and $\Lambda \in \mathbb{C}$ are piecewise-constants relating the response of the ring to the driving amplitude and frequency respectively, and we say

$$\Lambda = \begin{cases} \Lambda_N & \text{if } \theta > 1, \\ \Lambda_S & \text{if } \theta < 1, \end{cases} \quad \text{and} \quad s = \begin{cases} s_N & \text{if } \theta > 1, \\ s_S & \text{if } \theta < 1, \end{cases}\tag{5.2}$$

satisfying $\text{Re } \Lambda < 0$, and $s_N > s_S > 0$ (corresponding to physical values [10]). Thus we have a piecewise-smooth system about $\theta = 1$, with normal (N) and super (S) conducting modes, which we will denote by subscripts $r = N, S$. The constant g describes the efficiency of heat transfer with the microbridge, and has a large positive value $g \gg s/|\Lambda|^2$, as a result of which the system separates into 'slow' dynamics, in the neighbourhood of the surfaces where $\dot{\theta} = 0$ (parabolas $g\theta = s|\beta|^2$), and 'fast' dynamics towards these surfaces. This is illustrated in figure 5.1(i).

The theory of normally hyperbolic manifolds for singularly perturbed systems cannot be applied around the switching manifold $\theta = 1$, because the vector field is discontinuous. The theory of Filippov systems has so far made little progress in describing the bifurcations of equilibria for flows in more than two dimensions, though importantly, general results for periodic orbits do exist in the form of *discontinuity mappings* [5].

In [10], a Filippov model was derived from equation (5.1) by approximating the slow parabolas $\dot{\theta} = 0$ as switching manifolds in a manner consistent with section 2, see figure 5.1(i). The resulting piecewise-linear model contains a stable periodic orbit, which is destroyed in a catastrophic grazing-sliding bifurcation, figure ??(v), consistent with experimental observations. Here we use the hybrid sliding formulation to derive both a more complete bifurcation sequence for the nonsmooth system, and the qualitative dynamics they represent in a fully smooth, nonlinear model. This provides the bifurcations that should be sought in numerical analysis of a regularisation of the system, for example to use continuation analysis

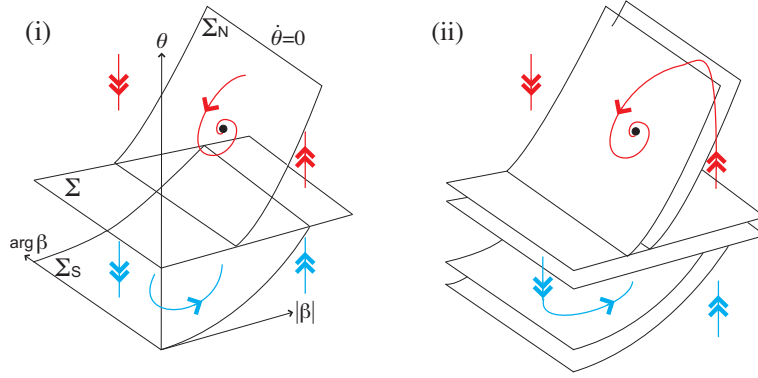


FIG. 5.1. Dynamics of the superconducting resonator. (i) Switching manifold Σ at $\theta = 1$ between normal and superconducting modes. The slow stable surfaces $\Sigma_{N,S}$ which become switching manifolds in the Filippov approximation. (ii) The hybrid sliding system, where pinch zones replace the switching manifolds.

packages such as AUTO [6]. figure 5.1(ii) shows the three pinch zones of the hybrid sliding system.

figure 5.2 shows two sliding bifurcations. (i) shows the catastrophic grazing-sliding bifurcation from figure ??(v), proposed in [10] to destroy a stable periodic orbit in the Filippov system. (ii) shows the switching-sliding bifurcation, as in figure ??(iii), for an unstable periodic orbit, which we will now propose also plays a part in the experimental observations.

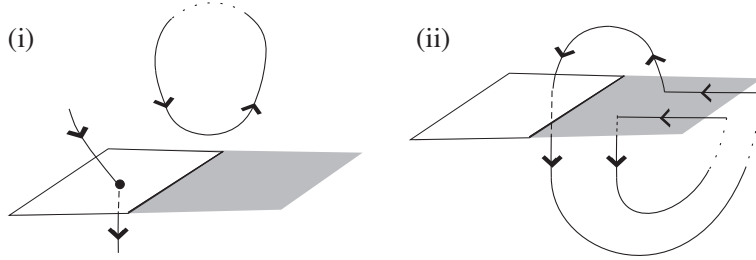


FIG. 5.2. (i) Catastrophic grazing-sliding bifurcation of a stable periodic orbit. (ii) Switching-sliding bifurcation of an unstable periodic orbit. The sliding regions (shaded) are unstable. The dotted paths represent an arbitrary return mechanism.

We begin by identifying any fixed points in the hybrid sliding system. From the results of section 2, we know that it is sufficient to consider a hybrid system approximating (5.1), and possessing the same fixed points. The hybrid system has four regions over which the vector field is smooth, separated by three switching manifolds

$$\begin{aligned}\Sigma_N &= \{(\beta, \theta) : h_N(\beta, \theta) = -\theta + s_N |\beta|^2 / g = 0\} \\ \Sigma_S &= \{(\beta, \theta) : h_S(\beta, \theta) = -\theta + s_S |\beta|^2 / g = 0\} \\ \Sigma &= \{(\beta, \theta) : \theta = 1\}\end{aligned}\tag{5.3}$$

Regarding the vector field outside these surfaces, we have

LEMMA 5.1. *There are no fixed points $\dot{\beta} = \dot{\theta} = 0$ outside the surfaces $\Sigma, \Sigma_N, \Sigma_S$.*

Proof. Outside the surfaces $\Sigma, \Sigma_N, \Sigma_S$, the θ component of the vector field is $\dot{\theta} = h_r(\beta, \theta)$, but by the definition of $\Sigma_{N,S}$, (5.3), this never vanishes outside Σ_N or Σ_S . \square

Following section 2, consider a strip $|h_r| < \sigma$, then a suitable choice for the thickness of the pinch zone is $\sigma = 1/g$. Now approximate the vector field as

$$\begin{pmatrix} \dot{\beta} \\ \dot{\theta} \end{pmatrix} \approx \begin{pmatrix} \Lambda_r \beta - i \\ \text{sgn } h_r \end{pmatrix} \quad (5.4)$$

taking $r = N$ for $\theta > 1$ and $r = S$ for $\theta < 1$. On Σ_N and Σ_S the sliding vector field (2.8) can be specified simply by taking

$$\dot{\beta} = \Lambda_r \beta - i \quad \text{where } h_r = 0. \quad (5.5)$$

LEMMA 5.2. (i) A stable focus exists on Σ_N if and only if $h_N(\frac{i}{\Lambda_N}, 1) > 0$.

(ii) A stable focus exists on Σ_S if and only if $h_S(\frac{i}{\Lambda_S}, 1) < 0$.

Proof. From (5.5), a fixed point $\dot{\beta} = 0$ of the sliding vector field on Σ_r , occurs where $\beta = \beta_r^{eq} = i/\Lambda_r$. On Σ_r we have $h_r(\beta, \theta) = 0$, and therefore $\theta_r^{eq} = s_r/(g|\Lambda_r|^2)$. The solution $(\beta_r^{eq}, \theta_r^{eq})$ is admissible only if it lies on Σ_r , that is, $\beta_r^{eq} \in \Sigma_N$ if and only if $\theta_N^{eq} > 1$, equivalent to $h_N(i/\Lambda_N, 1) > 0$, and $\beta_S^{eq} \in \Sigma_S$ if and only if $\theta_S^{eq} < 1$, equivalent to $h_S(i/\Lambda_S, 1) < 0$. Both of these are stable foci because the multiplier of $\text{Re}\beta$ in (5.5) is $\text{Re}\Lambda_r < 0$. \square

The annulus $g/s_N < |\beta|^2 < g/s_S$ on Σ is a region of unstable sliding. The linear approximation (5.4) is not accurate enough to capture correctly fixed points on Σ , and we must return to (5.1) to find the sliding vector field there, which from (2.8) is

$$\begin{pmatrix} \dot{\beta} \\ \dot{\theta} \end{pmatrix} = \begin{pmatrix} \frac{\Lambda_N h_S(\beta, 1) - \Lambda_S h_N(\beta, 1)}{h_S(\beta, 1) - h_N(\beta, 1)} \beta - i \\ 0 \end{pmatrix} \quad \text{if } \theta = 1, \quad \frac{g}{s_N} < |\beta|^2 < \frac{g}{s_S}. \quad (5.6)$$

For our purposes, it is enough to remark that a fixed point, by the definition of a sliding vector field, occurs at a point where the vector fields above and below Σ are antiparallel. From this we have:

LEMMA 5.3. The number of zeros of the unstable sliding vector field on Σ is

$$1 \quad \text{if } h_N(\Lambda_N, 1)h_S(\Lambda_S, 1) < 0, \quad (5.7)$$

$$0 \quad \text{if } h_N(\Lambda_N, 1)h_S(\Lambda_S, 1) > j^2/|\Lambda_N \Lambda_S|^2 > 0, \quad (5.8)$$

$$0 \quad \text{if } h_N(\Lambda_N, 1)h_S(\Lambda_S, 1) > 0, \quad \text{and } j/|\Lambda_S|^2 h_S(\Lambda_S, 1) > 0, \quad (5.9)$$

$$2 \quad \text{if } j^2/|\Lambda_N \Lambda_S|^2 > h_N(\Lambda_N, 1)h_S(\Lambda_S, 1) > 0 \quad \text{and } j/|\Lambda_S|^2 h_S(\Lambda_S, 1) < 0, \quad (5.10)$$

where $j = \frac{s_S + s_N}{2g} - \text{Re}[\Lambda_N \Lambda_S^*]$.

Proof. The upper (N) and lower (S) vector fields are antiparallel on Σ if there exists $\lambda < 0$ such that

$$\begin{pmatrix} \Lambda_N \beta - i \\ -g + s_N |\beta|^2 \end{pmatrix} = \lambda \begin{pmatrix} \Lambda_S \beta - i \\ -g + s_S |\beta|^2 \end{pmatrix}. \quad (5.11)$$

From the first component, for any valid solution of λ there is a unique zero at $\beta = i(\lambda - 1)/(\lambda \Lambda_S - \Lambda_N)$. Eliminating β from the simultaneous equations (5.11) gives

$$\lambda = \frac{j \pm \sqrt{j^2 - |\Lambda_N \Lambda_S|^2 h_N(\frac{i}{\Lambda_N}, 1) h_S(\frac{i}{\Lambda_S}, 1)}}{|\Lambda_S|^2 h_S(\frac{i}{\Lambda_S}, 1)}. \quad (5.12)$$

Real positive solutions of (5.12) occur in the numbers given by (5.7)-(5.10), and each real positive solution corresponds to a zero of the unstable sliding vector field. \square

LEMMA 5.4. *The number of fixed points in the system is either 1 or 3.*

Proof. By Lemma 5.3, there is a single fixed point on Σ when $h_N(\Lambda_N, 1)h_S(\Lambda_S, 1) < 0$. Then either $h_N(\Lambda_N, 1) > 0 > h_S(\Lambda_S, 1)$, in which case by Lemma 5.2 there are two other fixed points, one on each of Σ_N and Σ_S , or $h_N(\Lambda_N, 1) < 0 < h_S(\Lambda_S, 1)$, in which case by Lemma 5.2 there are no fixed points on Σ_S or Σ_N ; hence there are either 3 or 1 fixed points. There are either 2 or 0 fixed points on Σ when $h_N(\Lambda_N, 1)h_S(\Lambda_S, 1) < 0$, then $h_N(\Lambda_N, 1)$ and $h_S(\Lambda_S, 1)$ have the same sign, in which case by Lemma 5.2 there is one other fixed point on either Σ_S or Σ_N ; hence there are either 3 fixed points. Finally by Lemma 5.1 there are no fixed points outside of $\Sigma, \Sigma_N, \Sigma_S$, so the result follows. \square

Equilibria can only appear/disappear in the sliding regions in two ways, given by the following two lemmas:

LEMMA 5.5. *A saddle-node bifurcation takes place on Σ when $h_N(\Lambda_N, 1)h_S(\Lambda_S, 1) = j^2/|\Lambda_N\Lambda_S|^2$.*

Proof. If we vary the parameters Λ or s such that $j^2 - |\Lambda_N\Lambda_S|^2h_N(\Lambda_N, 1)h_S(\Lambda_S, 1)$ changes sign then, by Lemma 5.3, the number of fixed points on the unstable sliding vector field on Σ jumps between 0 and 2. Since the sliding vector field is smooth inside its domain $g/s_N < |\beta|^2 < g/s_S$ on Σ , this constitutes a saddle-node bifurcation [13]. \square

LEMMA 5.6. *Equilibria pass continuously between Σ and either Σ_N or Σ_S , respectively when $h_N(\frac{i}{\Lambda_N}, 1) = 0$ or $h_S(\frac{i}{\Lambda_S}, 1) = 0$.*

Proof. Let $h_N(i/\Lambda_N, 1)h_S(i/\Lambda_S, 1) < 0$ and $h_N(i/\Lambda_N, 1) < 0$, then the only fixed point in the system is on Σ . As $h_N(i/\Lambda_N, 1)$ changes sign, a fixed point appears on Σ_N by Lemma 5.2, and assuming generically that $h_S(i/\Lambda_S, 1) \neq 0$, then $h_N(i/\Lambda_N, 1)h_S(i/\Lambda_S, 1)$ changes sign, so by Lemma 5.3 the fixed point on Σ vanishes. To state that a fixed point has passed from Σ to Σ_N , it remains to show that the fixed point disappeared from Σ and appeared in Σ_N at the same coordinates. The transition takes place when $h_N(i/\Lambda_N, 1) = 0$, which means the fixed point in Σ_N lies on the boundary with the unstable sliding region on Σ , therefore $h_N(\beta, 1) = 0$ and $\beta = i/\Lambda_N$. From (5.6), the unstable sliding vector field at that point is $\dot{\beta} = 0$, hence the fixed points on Σ and Σ_N coincide at transition. The argument for fixed points passing from Σ to Σ_S when $h_S(i/\Lambda_S, 1) = 0$ is analogous. \square

We must then ask whether it makes sense for a fixed point to pass from Σ to Σ_N or Σ_S , since sliding is unstable on Σ but stable on Σ_N and Σ_S . In the absence of any theorems of nonsmooth systems to answer this question, the resolution to the disparity is the following.

We propose to relate the fixed points to each other by assuming that the nonsmooth model (5.1)-(5.2) is an approximation to a hybrid sliding system as in section 2. Then, by Theorem 2.1, each fixed point in the Lemmas above corresponds to a zero of some smooth three dimensional vector field. If the smooth system is generic, the number of fixed points must either be conserved, or annihilate in pairs via saddle-node bifurcations [13]; note that no such result has been proven for three dimensional Filippov systems. By considering the total number of fixed points in the stable sliding regions on Σ_N and Σ_S , and in the unstable sliding region on Σ , we have:

PROPOSITION 5.7. *The transition of a fixed point between switching manifolds in Lemma 5.6, takes place via a Hopf bifurcation.*

Proof. We give only a heuristic argument for this proposition, which we will verify by simulation. A sliding fixed point has eigenvalues $\{e_1, e_2, e_3\}$, one of which is infinite due to the infinite (in)stability of the switching manifold it inhabits. Without loss of generality let $e_1 \rightarrow \pm\infty$. Assuming the nonsmooth system is a hybrid sliding approximation to some smooth vector field, this corresponds to a fixed point in the smooth system with eigenvalues

$\{e'_1, e'_2, e'_3\}$ where $|\text{Re}(e'_1)| \gg 1$. If the fixed point lies on Σ_N or Σ_S , then all three eigenvalues have negative real parts, while on Σ , at least one of the eigenvalues has a positive real part, $e_1 \rightarrow \infty$. This implies that at least one eigenvalue crosses the imaginary axis, which by the Andronov-Hopf theorem [13] generically implies that the fixed point in the smooth system undergoes a Hopf bifurcation. \square

As in section 3.2, this is not the only possible solution, but it is the simplest, and we can ask what it implies about the system. A Hopf bifurcation suggests that, close to the transition, a periodic orbit exists in the neighbourhood of the fixed point. This is only possible if the orbit passes through Σ , implying that it is unstable in one direction. It must also pass through the region Σ_N or Σ_S (whichever the fixed point moves to), implying that it is stable in one direction. Therefore the periodic orbit is of saddle type, and it is easy to verify that this means it exists when the fixed point is on Σ_N or Σ_S , and that the Hopf bifurcation is therefore subcritical.

figure 5.3 shows a possible form for such a discontinuity-induced Hopf bifurcation, in which a saddle fixed point on Σ becomes a stable focus on Σ_N , and develops a saddle-type periodic orbit.

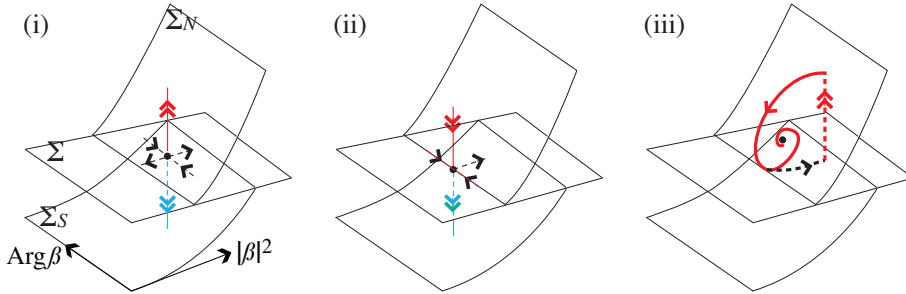


FIG. 5.3. A nonsmooth Hopf bifurcation in the resonator model. (i) a saddlepoint of unstable sliding lies on Σ . (ii) the saddlepoint at the boundary between Σ and Σ_N . (iii) the fixed point becomes a stable focus of sliding on Σ_N , surrounded by a saddle-type periodic orbit.

figure 5.4 shows a numerical simulation of (5.1), confirming that such a bifurcation is indeed observed in the nonsmooth system.

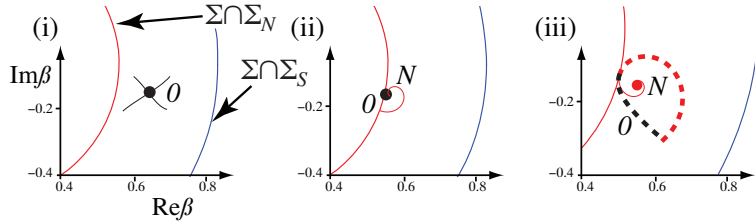


FIG. 5.4. Simulation of the system (5.1) shown in the β plane. Orbits are labeled $N, S, 0$ corresponding to whether they lie on Σ_N, Σ_S or Σ . Parameters are $s_n = 3.891g$, $s_S = 1.297g$, $\Lambda_S = -0.2 + i$, $\Lambda_N = -0.5 + ia$ with: (a) $a = 2.2$, showing a saddle on Σ_0 , (b) $a = 1.9$, showing a fixed point on the boundary, (c) $a = 1.7$, showing a stable saddle on Σ_N and a periodic orbit with an unstable segment on Σ_N and stable segment on Σ .

Now consider what happens as the periodic orbit in figure 5.3 grows. Eventually it may intersect the boundary between Σ and Σ_S as in figure 5.5(ii), and in doing so it can develop a segment on Σ_S , figure 5.5(iii). This is the switching-sliding bifurcation of a saddle-type periodic orbit, Fig. 5.2(ii), where the return mechanism involves traversing stable and unstable

sliding switching manifolds. figure 5.6 confirms that this occurs in the simulation as $\text{Im}\Lambda_N$ varies.

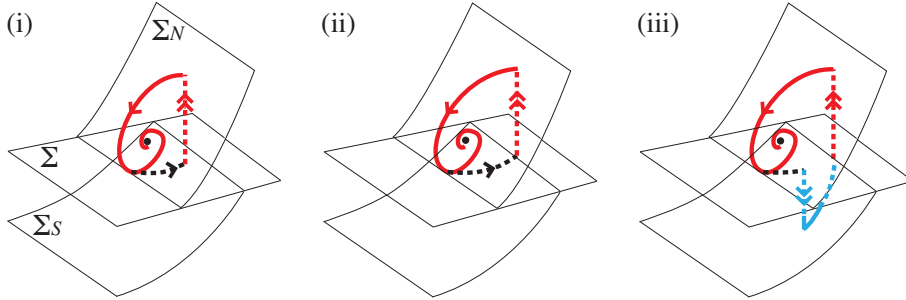


FIG. 5.5. The switching-sliding bifurcation of a piecewise-smooth saddle-type periodic orbit. From (i) to (iii) the periodic orbit grows and develops a segment jumping off Σ to stable sliding on Σ_S .

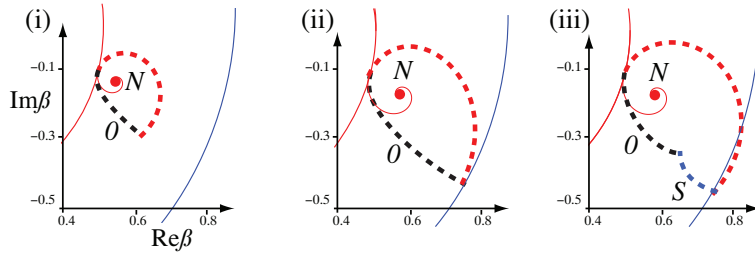


FIG. 5.6. Simulation continued from figure 5.4 where $\Lambda_N = -0.5 + ix$ with: (a) $x = 1.6$, (b) $x = 1.58$, (c) $x = 1.573$. The periodic orbit gains a segment on Σ_S via a switching-sliding bifurcation.

Simulations reveal a second, stable periodic orbit in the system, which has been omitted from figures 5.3-5.5 for clarity, but we now shown in figure 5.7. The experiments that motivated this model [20], and previous analysis on the nonsmooth model [10], reveal a stable periodic orbit that suddenly vanishes from the system as a parameter is varied continuously. An explanation for this was provided for this in the nonsmooth model [10], with existence conditions, in terms of the catastrophic grazing-sliding bifurcation, figure 5.2(i). It was not explained how the catastrophic nature of the disappearance is to be understood, however, and we can now provide the explanation.

The saddle periodic orbit in figure 5.5(iii) or figure 5.7(i) visits all three sliding regions on Σ , Σ_N , and Σ_S , while the stable periodic orbit visits only the stable regions on Σ_N and Σ_S , shown in figure 5.7(i). The stable orbit shrinks and develops a tangency to the boundary between Σ and Σ_N , while the saddle orbit grows, its segment in Σ shrinking to zero until it jumps off Σ from the tangency point. At this instant, figure 5.7(ii), the two periodic orbits coincide, and under further parameter variation to figure 5.7(iii) they vanish via a saddle-node bifurcation of periodic orbits. The simulation confirming this is shown in figure 5.8.

In this instance, then, the catastrophic sliding bifurcation has an interpretation as a saddle-node bifurcation, involving a periodic orbit that has directions of infinite stability and instability that alternate over its period.

Note that in the nonsmooth system, it is not clear that we can refer to the periodic orbits as saddle type or stable, and the saddle-node bifurcation of such periodic orbits has not been defined. Nor is there a clear means to fill these holes in the theory concerning vector fields

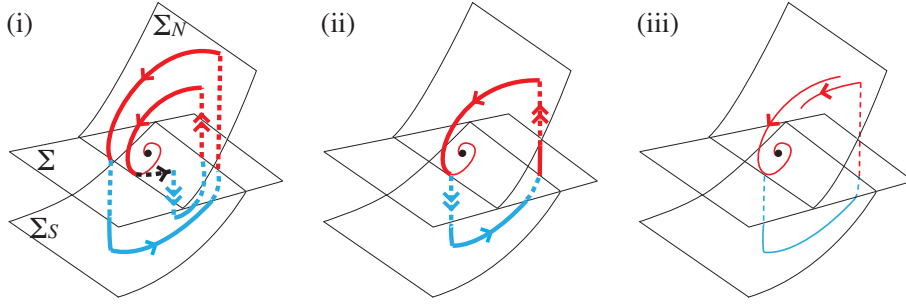


FIG. 5.7. Saddle-node bifurcation of periodic orbits in the resonator. (i) a stable periodic orbit surrounds a saddle periodic orbit. (ii) the two orbits coalesce by forming a tangency to Σ , at which the forward evolution is nonunique – a solution could follow the periodic orbit or slide into the focus. (iii) all solutions slide towards a stable focus.

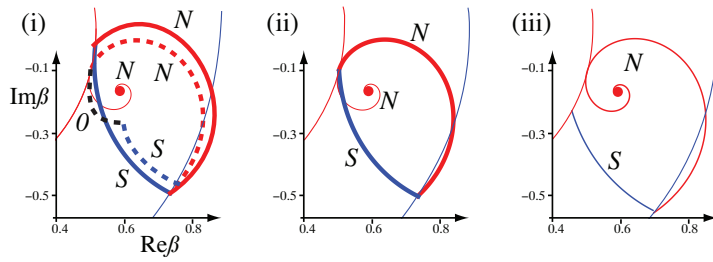


FIG. 5.8. Simulation continued from figure 5.6 where $\Lambda_N = -0.5 + ix$ with: (a) $x = 1.572$, (b) $x = 1.57$, (c) $x = 1.56$. An orbit with stable and unstable segments coalesces with a stable periodic orbit (omitted from Figs. 5.4-5.6 for clarity), and vanish via catastrophic grazing-sliding.

which are discontinuous. However, by interpreting this as the hybrid sliding approximation of a smooth system, we have recourse to well defined concepts, and we have shown that these can be used consistently to derive a plausible mechanism for experimental observations, which we have verified above by simulation.

This is one possible mechanism by which a stable periodic orbit could be destroyed. Another possibility is that it forms a homoclinic connection to a nodal point on the crossing region of Σ . This can be investigated in a similar manner, using the hybrid sliding formalism to understand how bifurcations in the nonsmooth system are related to well-known bifurcations in smooth systems. As yet the argument for this scenario is purely topological, and the parameters at which it may occur have not been identified.

6. Concluding Remarks. The geometrical analysis in section ?? provides a means to understand how bifurcations in a smooth dynamical model relate to those in a nonsmooth approximation of it. These results therefore allow a study of a system's simplified nonsmooth model, forming a basis for simulations, numerical continuation, and singular perturbation analysis on the smooth system.

We observed in section ?? that a bifurcation in a smooth system and its corresponding hybrid system are separated in parameter space by a distance depending on σ , the size of the pinch zone. In , a nonsmooth analogue of the Hopf bifurcation takes place when $x_\Sigma = \sigma$ provided that $\alpha < 4\sigma^2$. In figure ?? we see that a nonsmooth analogue of the Hopf bifurcation also takes place along the curve $x_\Sigma = -\sigma + \sqrt{\alpha}$ for $x_\Sigma < \sigma$, and along $\alpha \in (0, 4\sigma^2)$ for $x_\Sigma = \sigma$ (section ??). The effect of the pinch zone is particularly clear in the singular

perturbation problem in section 3.3, where a fixed point resides in the middle of the pinch zone (corresponding to $x_\Sigma = 0$). Then a Hopf bifurcation takes place at the parameter value $a = 1$ in the smooth system, but at $a = \sqrt{1 - \frac{1}{3}\sigma^2} \approx 1 - \frac{1}{6}\sigma^2$. A more general result on the size of perturbation caused by pinching would clearly be of interest, and will require a more general theory of the classes of functions and maps that together define a pinch zone and its mapping.

Sections ??-?? show that critical points in nonsmooth vector fields can be classified by combining different forms of pinching with the singularity theory of smooth vector fields. It suggests also that every bifurcation of a smooth vector field has a direct counterpart in nonsmooth systems, though the consequences are very different. The dynamics varies qualitatively depending on whether a bifurcation takes place within the pinch zone, and these differences are described by discontinuity induced bifurcations: periodic orbits enter the pinch zone by means of sliding bifurcations (section ??), whose classification was completed in [12], fixed points either cross the pinch zone or become sliding fixed points (section ??), and changes of stability lead to, for instance, nonsmooth Hopf bifurcations (section 3.3 and ??). The sliding bifurcations give a simple means to identify such complex behaviour as canards (section ??). Further study is required into the implications of invariant manifolds entering a pinch zone, and its effect on asymptotic stability and chaos.

During drafting this paper it has been noticed by M. Desroches that the canard phenomenon in section 3.2 appeared some years hence in the study of canards, in the guise of nonstandard analysis. The detailed role of this *catastrophic sliding bifurcation at a two-fold* is the subject of ongoing study.

We have presented the Filippov convention as a geometrical approximation to dynamical systems containing rapid variations of scale. The convex set (2.3) may be used in other ways, for example we can relax the condition (2.5), replace the sliding vector field with flux through the pinch zone, or choose the sliding vector field from $F(\xi)$ stochastically. Although the Filippov convention is shown to be one possible choice of hybrid sliding model, the wealth of literature on Filippov systems (see, for example [4, 15]) show it to be nonetheless a powerful analytical tool that we aim to sharpen with our more general analysis.

We have not discussed discontinuities at ‘corners’ explicitly, but in principal a pinch zone can be defined that has more complicated topology, such at the three intersecting slabs in the model of the superconducting resonator in section 5.

A smooth system, and a hybrid system derived from it (as in section 2), are semi-equivalent by definition. By this we mean that every orbit of the smooth system can be mapped to an orbit of the hybrid system, though noninvertibly. Based on this, we propose that a useful definition of structural stability of nonsmooth systems might be the following. Define two nonsmooth vector fields to be topologically equivalent (or semi-equivalent) if they can be derived, using equivalent pinch functions, from two smooth vector fields that are themselves topologically equivalent. Then we define a nonsmooth vector field to be structurally (semi-) stable if it is semi-equivalent to a structurally stable smooth vector field. A rigorous definition requires us to define an equivalence between pinch functions, which remains to be done. It also requires results on the stability of a vector field paired with a function, which was partially pre-empted by Teixeira [24].

REFERENCES

- [1] G. Bachar, E. Segev, O. Shtempluck, E. Buks, and S. W. Shaw. Noise induced intermittency in a superconducting microwave resonator. *arXiv:0810.0964*, 2008.
- [2] E. Benoît, J. L. Callot, F. Diener, and M. Diener. Chasse au canard. *Collect. Math.*, 31-32:37–119, 1981.

- [3] R. Casey, H. de Jong, and J. L. Gouze. Piecewise-linear models of genetic regulatory networks: Equilibria and their stability. *J.Math.Biol.*, 52:27–56, 2006.
- [4] M. di Bernardo, C. J. Budd, A. R. Champneys, and P. Kowalczyk. *Piecewise-Smooth Dynamical Systems: Theory and Applications*. Springer, 2008.
- [5] M. di Bernardo, P. Kowalczyk, and A. Nordmark. Bifurcations of dynamical systems with sliding: derivation of normal-form mappings. *Physica D*, 170:175–205, 2002.
- [6] E. J. Doedel, A. R. Champneys, T. F. Fairgrieve, Yu. A. Kuznetsov, B. Sandstede, and X. Wang. AUTO97: Continuation and bifurcation software for ordinary differential equations (with HomCont). *Technical report, Concordia University*, 1997.
- [7] W Eckhaus. Relaxation oscillations including a standard chase on French ducks. *Lect. Notes Math.*, 985:449–494, 1983.
- [8] N. Fenichel. Geometric singular perturbation theory. *J. Differ. Equ.*, 31:53–98, 1979.
- [9] A. F Filippov. *Differential Equations with Discontinuous Righthand Sides*. Kluwer Academic Publishers, Dordrecht, 1998.
- [10] M. R. Jeffrey, A. R. Champneys, M. di Bernardo, and S. W. Shaw. Catastrophic sliding bifurcations and onset of oscillations in a superconducting resonator. *Phys. Rev. E*, 81(1):016213–22, 2010.
- [11] M. R. Jeffrey and A. Colombo. The two-fold singularity of discontinuous vector fields. *SIAM Journal on Applied Dynamical Systems*, 8(2):624–640, 2009.
- [12] M. R. Jeffrey and S. J. Hogan. The geometry of generic sliding bifurcations. *SIREV*, submitted 2009.
- [13] Y. A. Kuznetsov. *Elements of Applied Bifurcation Theory*. Springer, 2nd Ed., 1998.
- [14] Yu. A. Kuznetsov, S. Rinaldi, and A. Gragnani. One-parameter bifurcations in planar Filippov systems. *Int.J.Bif.Chaos*, 13:2157–2188, 2003.
- [15] R. I. Leine and N. Henk. *Dynamics and Bifurcations of Non-Smooth Mechanical Systems*. Springer, 2004.
- [16] J. Llibre, P. R. da Silva, and M. A. Teixeira. Sliding vector fields via slow-fast systems. *Bull. Belg. Math. Soc. Simon Stevin*, 15(5):851–869, 2008.
- [17] K. Popp and P. Stelter. Stick slip vibrations and chaos. *Phil. Trans. Roy. Soc. A*, 332(1624):89–105, 1990.
- [18] E. Segev, B. Abdo, O. Shtempluck, and E. Buks. Extreme nonlinear phenomena in NbN superconducting stripline resonators. *Physics Letters A*, 366(1-2):160 – 164, 2007.
- [19] E. Segev, B. Abdo, O. Shtempluck, and E. Buks. Novel self-sustained modulation in superconducting stripline resonators. *EPL*, 78(5):57002 (5pp), 2007.
- [20] E. Segev, B. Abdo, O. Shtempluck, and E. Buks. Thermal instability and self-sustained modulation in superconducting NbN stripline resonators. *J. Phys: Condens. Matter*, 19(9):096206(14pp), 2007.
- [21] S. N. Simić, K. H. Johansson, J. Lygeros, and S. Sastry. Structural stability of hybrid systems. *European Control Conference*, pages 3858–3863, 2001.
- [22] S. N. Simić, K. H. Johansson, J. Lygeros, and S. Sastry. Towards a geometric theory of hybrid systems. *Dyanmics of Continuous, Discrete and Impulsive Systems, Series B*, 12(5-6):649–687, 2005.
- [23] P. Szmolyan and M. Wechselberger. Canards in \mathbb{R}^3 . *J. Differ. Equ.*, 177:419–453, 2001.
- [24] M. A. Teixeira. Structural stability of pairings of vector fields and functions. *Boletim da S.B.M.*, 9(2):63–82, 1978.
- [25] M. A. Teixeira. Stability conditions for discontinuous vector fields. *J. Differ. Equ.*, 88:15–29, 1990.
- [26] M. A. Teixeira, J. Llibre, and P. R. da Silva. Regularization of discontinuous vector fields on \mathbb{R}^3 via singular perturbation. *J.Dyn.Diff.Equat.*, 19(2):309–331, 2007.
- [27] V. I. Utkin. Variable structure systems with sliding modes. *IEEE Trans. Automat. Contr.*, 22, 1977.
- [28] M. Wechselberger. Existence and bifurcation of canards in \mathbb{R}^3 in the case of a folded node. *SIAM J. App. Dyn. Sys.*, 4(1):101–139, 2005.
- [29] S. Wolfram. *The Mathematica Book*. Cambridge University Press, 1996.